Analysis of Path loss exponent and shadowing on beam antenna calculating diversity and sensitivity for case scenario

[1]Vijay kumar Prajapat, [2]Pramod Sharma

[1]Research Scholar, [2]Principal
Department of Electronics and communication Engineering
Regional College for Education Research and Technology
Jaipur, India

***Abstract*: This work compares large -scale propagation path loss for use over entire microwave and millimeter-wave (mmWave) radio spectrum with a frequency-weighted path loss exponent. This is used in the design of fifth-generation wireless system in urban macro cell, urban microcell, and Indore office and shopping mall scenarios. Here compare the accuracy and sensitivity using measured data from 30 propagation measurement data sets from 2 to 75 GHZ in this work, the input files contain path loss values obtained with the "Wireless in site" ray tracer by Romcom. For the indoor scenario and for outdoor scenario. The indoor scenario refers to a customizable conference room and bedroom in which removed furniture and electronic equipments hence the name "complex", "Semi complex" and "Simple". The outdoor vehicles to infrastructure (V2I) NLOS communication scenario is based on two types of horn antennas and a constantly aligning mechanism between Tx and Rx antenna beams. Comparative analysis will be shown for path loss analysis using these scenarios using MATLAB Software.**

***Index Terms*: Millimeter wave, path loss models, prediction accuracy, 5G**

Introduction

I. INTRODUCTION

Antenna can be defined as " the transition between a guided EM wave and a free-space EM wave and vice-versa as we can see in Figure (1):

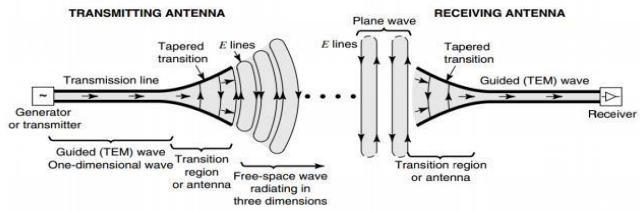

Fig. 3.1. The antenna as a transition structure, for a transmitting antenna and for a receiving

Antenna can be made as a transmitter or as a receiver, it is reciprocal device, as shown in figure 3.1 an antenna represents the area of transition between free-space wave and guided wave. Thus, an antenna is a transducer or transition device, between a guided wave and free-space wave, or vice versa. The guiding device or transmission line can be either a coaxial line or a hollow pipe (waveguide).

The antenna system can be modeled as an electrical circuit, as in Figure 3.2 we can see A transmission-line Thevenin equivalent of the antenna system in the transmitting mode, where the source is represented by an ideal generator, the transmission line is represented by a line with characteristic impedance Z_c, and the antenna is represented by a load Z_A [$Z_A = (R_L + R_r) + jX_A$] connected to the transmission line. R_L is referred to the conduction and dielectric losses associated with the antenna structure so $R_L = R_c + R_d$ while R_r , is used to represent the radiation resistance, which represents radiation by the antenna. The reactance X_A is used to represent the imaginary part of the impedance associated with radiation by the antenna. The aim here is to transform all the energy from the generator to the to the radiation resistance R_r, but this is ideal case.

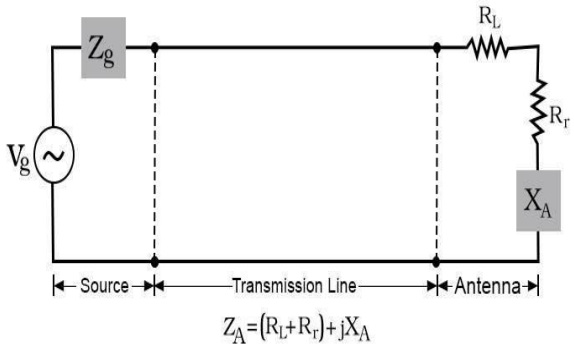

Fig. 3.2. Transmission- line Thevenin equivalent of antenna in transmitting mode

A. MAXWELL'S EQUATIONS

Electromagnetic theory is fundamental to understanding of microwave antennas and its present form was founded by James Clerk Maxwell (1831-1879), whose efforts led to the discovery of electromagnetic waves, the laws of electromagnetism that Maxwell put together in the form of four equations are presented in Table 3.1:

Table 3.1. Generalized Forms of Maxwell's Equations

Differential Form	Integral Form	Remarks
$\nabla \cdot \mathbf{D} = \rho_v$	$\oint \mathbf{D}.d\mathbf{S} = \oint \rho_v dv$	Gauss's law
$\nabla \cdot \mathbf{D} = 0$	$\oint \mathbf{B}.d\mathbf{S} = 0$	Nonexistence of isolated magnetic charge
$\nabla x\mathbf{E} = -\frac{\partial \mathbf{B}}{\partial t}$	$\oint \mathbf{E}.dI = -\frac{\partial \mathbf{B}}{\partial t}\int \mathbf{B}.d\mathbf{S}$	Faraday's law
$\nabla x\mathbf{H} = \mathbf{J} + \frac{\partial \mathbf{D}}{\partial t}$	$\oint \mathbf{H}.dI = \int \left(J + \frac{\partial D}{\partial t}\right).dS$	Ampere's circuit law

The first and the second are Gauss' laws for the electric and magnetic fields, the third is Faraday's law of induction, the forth is Ampere's law as amended by Maxwell to include the displacement current $\partial D/\partial t$.

$\partial \mathbf{D}/\partial t$ in Ampere's law is displacement current term which is essential in predicting the existence of propagating electromagnetic waves. The quantities E and H represent the electric and magnetic field intensities and are measured in units of [volt/m] and [ampere/m], respectively.

The quantities **D** and **B** are the electric and magnetic flux densities and are in units of [coulomb/m^2] and [weber/m^2], or [Tesla].

The quantities ρ and **J** are the volume charge density and electric current density (charge flux) of any external charges (that is, not including any induced polarization charges and currents.) They are measured in units of [coulomb/m^3] and [ampere/m^2]. The right-hand side of the second equation is zero because there are no magnetic monopole charges.

Radiators are written as "destined" (usually in the form of a rod or wire) in the form of a destined antenna by Webster's Dictionary to obtain or receive radio waves. Antenna is the transitional structure between free-space and a guiding device, as shown in Fig. 1.1. A navigation device or transmission line can take the form of a coaxial line or a hollow pipe (waveguide) and it is used to transfer electromagnetic energy from transmittance source to antenna or antenna to receiver. In the former case we have a transmitting antenna and later, a received antenna.

B. TYPES OF ANTENNAS

Now we will introduce and discuss some variations of different antenna types that will give a glimpse of what will happen in the rest of the book.

a. Wire Antennas
b. Aperture Antennas
c. Microstrip Antennas
d. Array Antennas
e. Reflector Antennas
f. Lens Antennas

C. ANTENNA PARAMETERS

In order to understand the performance of an antenna, definitions of various parameters are necessary, that are used to characterize the performance of an antenna when designing and measuring antennas. We can classify antenna parameters in to two kinds, first antenna parameters from the field point of view which include the radiation pattern, beam width, directivity, gain, polarization and

the bandwidth, and the second antenna parameters from the circuit point of view which include input impedance, radiation resistance, reflection coefficient, return loss, VSWR and bandwidth.

D. RADIATION PATTERN

The radiation pattern of an antenna is a plot of the radiated field/power as a function of the angle at a fixed distance, which should be large enough to be considered far field.

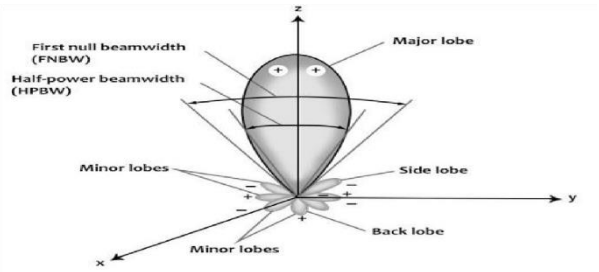

Fig. 3.3. Radiation lobes and beam widths of an antenna pattern

Since the radiation pattern is the variation of the radiated electric field over a sphere centered on the antenna, r is constant and we have only θ and φ variations of the field. We can normalize the field expression such that its maximum value is unity:

$$f(\theta,\phi) = \frac{E_\theta}{E_\theta(\max)} \quad (3.1)$$

Where $f(\theta,\varphi)$ is the normalized field pattern and E_θ (max) is the maximum value of the magnitude of E_θ over a sphere of radius r. Radiation Pattern Lobes can be classified into major or main, minor, side, and back lobes as shown in Figure 3.3, a major lobe (also called main beam) is defined as "the radiation lobe containing the direction of maximum radiation." A minor lobe is any lobe except a major lobe.

There are three common radiation patterns that are used to describe an antenna's radiation property:

Isotropic- An ideal lossless antenna having equal radiation in all directions, **Directional-** An antenna having the property of radiating or receiving electromagnetic waves more effectively in some directions than in others and **Omnidirectional-** An antenna having an essentially non directional pattern in a given plane and a directional pattern in any orthogonal plane. Directional or omnidirectional radiation properties are needed depending on the practical application. Omnidirectional patterns are normally desirable in mobile and hand-held systems.

E. BEAMWIDTH

The definition of beamwidth of an antenna pattern is the angular separation between two identical points on opposite side of the pattern maximum. There are a number of beamwidth in an antenna pattern. The Half-Power Beamwidth (HPBW) is the most important one, which is defined by IEEE as: "In a plane containing the direction of the maximum of a beam, the angle between the two directions in which the radiation intensity is one-half value of the beam", the First Null Beamwidth (FNBW) is defined as the angular separation between the first nulls of the pattern. Both the HPBW and FNBW are shown in Figure 3.3.

F. DIRECTIVITY

Directivity is very important antenna parameter which defined as the ratio of the radiation intensity in a given direction from the antenna to the radiation intensity averaged over all directions. The average radiation intensity is equal to the total power radiated by the antenna divided by 4π. Simply, the directivity of a nonisotropic source is equal to the ratio of its radiation intensity in a given direction over that of an isotropic source. In mathematical form, it can be written as

$$D = D(\theta,\phi) = \frac{U(\theta,\phi)}{U_0} = \frac{4\pi U(\theta,\phi)}{P_{rad}} \quad (3.2)$$

If the direction is not specified, it implies the direction of maximum radiation intensity (maximum directivity) expressed as:

$$D_{max} = D_0 = \frac{U_{max}}{U_0} = \frac{4\pi U_{max}}{P_{rad}} \quad (3.3)$$

Where,

D = directivity (dimensionless)

D_0= maximum directivity (dimensionless)

U = radiation intensity (W/unit solid angle)

U_{max} = maximum radiation intensity (W/unit solid angle)

U_0 = radiation intensity of isotropic source (W/unit solid angle)

P_{rad} = total radiated power (W)

G. MICROSTRIP ANTENNAS

In recent years Microstrip antennas have been one of the most important topics in antenna theory and design, and are increasingly used in a wide range of modern microwave systems. Microstrip "patch" antenna can be defined as that antenna which made from patches of conducting material on a dielectric substrate above a ground plane. Microstrip antennas are used because of their low cost, Low weight, low size, with simple feed.

• Microstrip Antenna Advantages and limitations:

Microstrip antenna has many benefits when comparing with other microwave antennas types. These advantages are:

- Low weight, low size, and thin profile configuration.
- Ease to design and fabricate.
- Low fabrication cost.
- Many designs readily produce linear or circular polarization Dual frequency and dual polarization can be achieved easily.
- Can easily conform to a curved surface of a vehicle or product.
- It is easy to be integrated with microwave integrated circuits.
- Feed lines and matching networks can be fabricated simultaneously with antenna structure.
- An array of microstrip antennas can be used to form a pattern that is difficult to synthesize using a single element.
- Smart antennas can be designed when microstrip antennas are combined with phase shifters or PIN-diode switches.

Disadvantages are:

- Narrow bandwidth (1%), while mobiles need (8%).
- Lower gain (~6 dB)
- Poor antenna efficiency.
- Sensitivity to environmental factors such as temperature and humidity.
- An array suffers presence of feed network decreasing efficiency.

II. RESULT AND ANALYSIS

Path loss formulas

$$\mathrm{PL}^{CIF}(f,d)[\mathrm{dB}] = \mathrm{FSPL}(f,1\,m)[\mathrm{dB}] + 10\log_{10}(d)\left(n(1-b)+\frac{nb}{f_0}f\right) + X_\sigma^{CIF} \quad (4.1)$$

$$X_\sigma^{CIF} = A - D(a+gf) \quad (4.2)$$

$$\sigma^{CIF} = \sqrt{\frac{\sum X_\sigma^{CIF2}}{N}} = \sqrt{\frac{\sum\left(A-D(a+gf)\right)^2}{N}} \quad (4.3)$$

$$\frac{\partial\sum\left(A-D(a+gf)\right)^2}{\partial a} = \sum 2D(aD+gDf-A) = 2(a\sum D^2 + g\sum D^2 f - \sum DA) = 0 \quad (4.4)$$

$$\frac{\partial\sum\left(A-D(a+gf)\right)^2}{\partial g} = \sum 2Df(aD+gDf-A) = 2(a\sum D^2 f + g\sum D^2 f^2 - \sum DAf) = 0 \quad (4.5)$$

Which can be simplified to

$$a\sum D^2 + g\sum D^2 f - \sum DA = 0 \quad (4.6)$$

$$a\sum D^2 f + g\sum D^2 f^2 - \sum DAf = 0 \quad (4.7)$$

$$a = \frac{\sum D^2 f \sum DAf - \sum D^2 f^2 \sum DA}{(\sum D^2 f)^2 - \sum D^2 \sum D^2 f^2} \quad (4.8)$$

$$g = \frac{\sum D^2 f \sum DA - \sum D^2 \sum DAf}{(\sum D^2 f)^2 - \sum D^2 \sum D^2 f^2} \quad (4.9)$$

$$n = a + gf_0 \quad (4.10)$$

$$b = \frac{gf_0}{a+gf_0} \quad (4.11)$$

A. Bedroom Scenario

Condition 1: Complex Bedroom Scenario

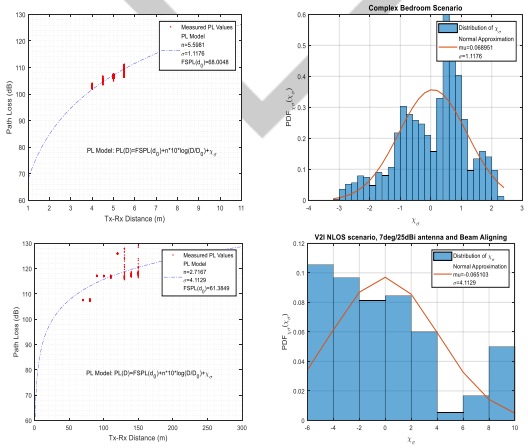

Fig. 4.1. Complex Bedroom Scenario with V2I NLOS scenario, 7deg/25dBi antenna and Beam Aligning

Fig.4.1 represents four graphical output analysis of Complex bedroom scenario with outdoor vehicle to infrastructure (V2I) NLOS communication scenario and 7 deg/ 25 dBi antenna as beam aligning. The analysis of observation data for the condition shows path loss parameter as $n = 5.5981.5981\sigma = 1.117676$nd $d_O = 68.0048$ at T_X-R_X distance. For bedroom scenario distribution of x_σ gives $mu = 0.06895151$nd $\sigma = 1.1176$. for V2I condition measured PL values are $n = 2.7167.7167\sigma = 4.112929$nd $d_O = 61.3846$ similarly for beam aligning antenna $mu = 0.06510303$nd $\sigma = 4.1129$.

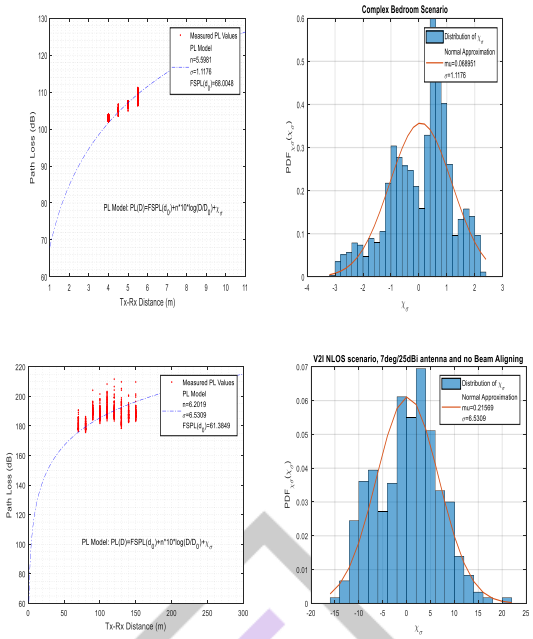

Fig.4.2. Complex Bedroom Scenario with V2I NLOS scenario, 7deg/25dBi antenna and no Beam Aligning

Fig.4.2 represents four graphical output analysis of Complex bedroom scenario with outdoor vehicle to infrastructure (V2I) NLOS communication scenario and 7 deg/ 25 dBi antenna as no beam aligning. The analysis of observation data for the condition shows path loss parameter as $n = 5.5981.5981\sigma = 1.117676$nd $d_o = 68.0048$ at Tx-Rx distance. For bedroom scenario distribution of x_σ gives $mu = 0.06895151$nd $\sigma = 1.1176$. For V2I condition measured PL values are $n = 6.2019.2019\sigma = 6.530909$nd $d_o = 61.3846$ similarly for no beam aligning antenna $mu = 0.2156969$nd $\sigma = 6.5309$.

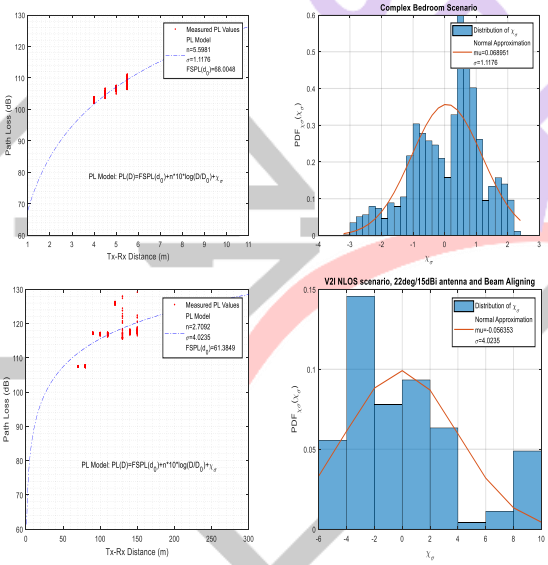

Fig. 4.3. Complex Bedroom Scenario with V2I NLOS scenario, 22deg/15dBi antenna and Beam Aligning

Fig.4.3 represents four graphical output analysis of Complex bedroom scenario with outdoor vehicle to infrastructure (V2I) NLOS communication scenario and 22 deg/ 15 dBi antenna as beam aligning. The analysis of observation data for the condition shows path loss parameter as $n = 5.5981.5981\sigma = 1.117676$nd $d_o = 68.0048$ at Tx-Rx distance. For bedroom scenario distribution of x_σ gives $mu = 0.06895151$nd $\sigma = 1.1176$. For V2I condition measured PL values are $n = 2.7092.7092\sigma = 4.023535$nd $d_o = 61.3846$ similarly for beam aligning antenna $mu = 0.05635353$nd $\sigma = 4.0235$.

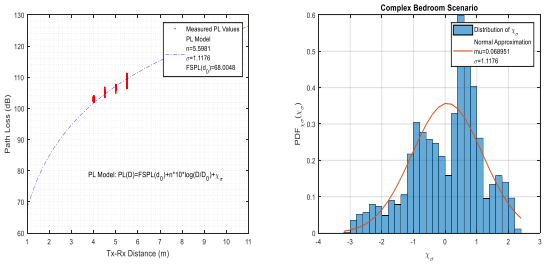

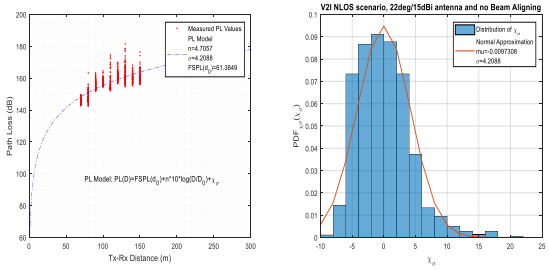

Fig. 4.4. Complex Bedroom Scenario with V2I NLOS scenario, 22deg/15dBi antenna and no Beam Aligning

Fig.4.4 represents four graphical output analysis of Complex bedroom scenario with outdoor vehicle to infrastructure (V2I) NLOS communication scenario and 22 deg/ 15 dBi antenna as no beam aligning. The analysis of observation data for the condition shows path loss parameter as $n = 5.5981.5981\sigma = 1.117676$nd $d_o = 68.0048$ at T_X-R_X distance. For bedroom scenario distribution of x_σ gives $mu = 0.06895151$nd $\sigma = 1.1176$. For V2I condition measured PL values are $n = 4.7057.7057\sigma = 4.208888$nd $d_o = 61.3846$ similarly for no beam aligning antenna $mu = 0.009730808$nd $\sigma = 4.2088$.

Condition 2: Semi Complex Bedroom Scenario

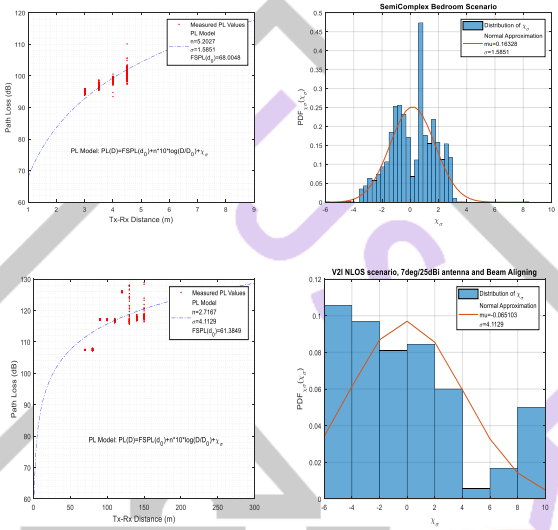

Fig.4.5. Semi Complex Bedroom Scenario with V2I NLOS scenario, 7deg/25dBi antenna and Beam Aligning

Fig.4.5 represents four graphical output analysis of semi complex bedroom scenario with outdoor vehicle to infrastructure (V2I) NLOS communication scenario and 7 deg/ 25 dBi antenna as beam aligning. The analysis of observation data for the condition shows path loss parameter as $n = 5.2027.2027\sigma = 1.585151$nd $d_o = 68.0048$ at T_X-R_X distance. For bedroom scenario distribution of x_σ gives $mu = 0.1632828$nd $\sigma = 1.5851$. for V2I condition measured PL values are $n = 2.7167.7167\sigma = 4.112929$nd $d_o = 61.3846$ similarly for beam aligning antenna $mu = 0.06510303$nd $\sigma = 4.1129$.

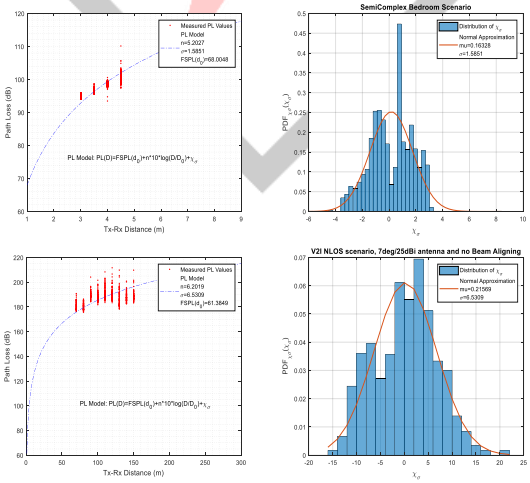

Fig. 4.6. Semi Complex Bedroom Scenario with V2I NLOS scenario, 7deg/25dBi antenna and no Beam Aligning

Fig.4.6 represents four graphical output analysis of Semi Complex bedroom scenario with outdoor vehicle to infrastructure (V2I) NLOS communication scenario and 7 deg/ 25 dBi antenna as no beam aligning. The analysis of observation data for the condition shows path loss parameter as $n = 5.2027.2027\sigma = 1.585151$nd $d_o = 68.0048$ at T_X-R_X distance. For bedroom scenario distribution of x_σ gives $mu = 0.1632828$nd $\sigma = 1.5851$. for V2I condition measured PL values are $n = 6.2019.2019\sigma = 6.530909$nd $d_o = 61.3846$ similarly for beam aligning antenna $mu = 0.2156969$nd $\sigma = 6.5309$.

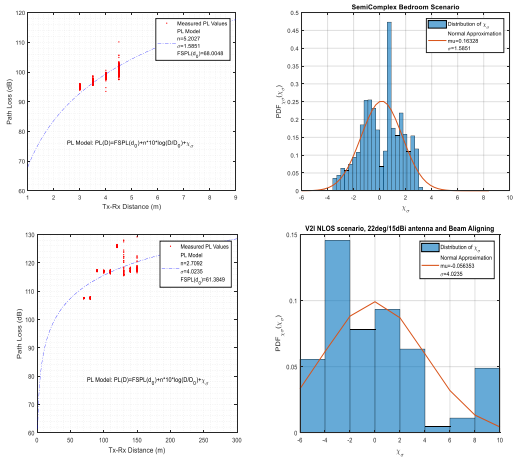

Fig. 4.7. Semi Complex Bedroom Scenario with V2I NLOS scenario, 22deg/15dBi antenna and Beam Aligning

Fig.4.7 represents four graphical output analysis of Semi Complex bedroom scenario with outdoor vehicle to infrastructure (V2I) NLOS communication scenario and 22 deg/ 15 dBi antenna as beam aligning. The analysis of observation data for the condition shows path loss parameter as $n = 5.2027 .2027 \sigma = 1.585151$nd $d_o = 68.0048$ at T_X-R_X distance. For bedroom scenario distribution of x_σ gives $mu = 0.1632828$nd $\sigma = 1.5851$. For V2I condition measured PL values are $n = 2.7092 .7092 \sigma = 4.023535$nd $d_o = 61.3846$ similarly for beam aligning antenna $mu = 0.05635353$nd $\sigma = 4.0235$.

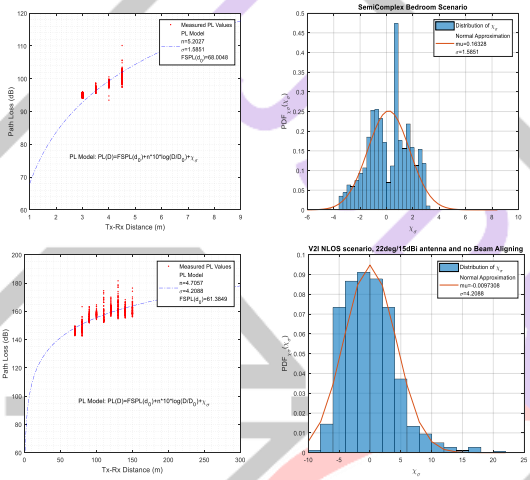

Fig. 4.8. Semi Complex Bedroom Scenario with V2I NLOS scenario, 22deg/15dBi antenna and no Beam Aligning

Fig.4.8 represents four graphical output analysis of Semi Complex bedroom scenario with outdoor vehicle to infrastructure (V2I) NLOS communication scenario and 22 deg/ 15 dBi antenna as no beam aligning. The analysis of observation data for the condition shows path loss parameter as $n = 5.2027 .2027 \sigma = 1.585151$nd $d_o = 68.0048$ at T_X-R_X distance. For bedroom scenario distribution of x_σ gives $mu = 0.1632828$nd $\sigma = 1.5851$. for V2I condition measured PL values are $n = 4.7057 .7057 \sigma = 4.208888$nd $d_o = 61.3846$ similarly for beam aligning antenna $mu = 0.009730808$nd $\sigma = 4.2088$.

III. DIVERSITY

(A) Equal Gain Combining

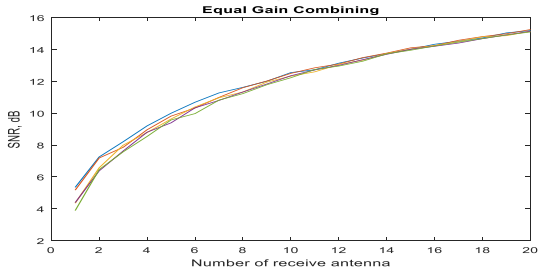

Fig. 4.17. Diversity of antenna with equal Gain Combining and SNR

(B) MRC

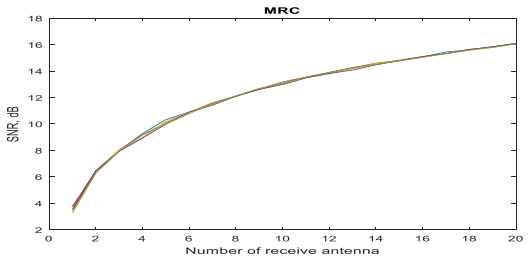

Fig. 4.18. Diversity of antenna with MRC and SNR

Fig. 4.17 shows the diversity of antenna beam for equal gain combining (EGC) and SNR ratings. It represents that as number of receiving antenna increases SNR value get less path loss as when number of antenna are less. Where as in fig 4.18, it is represented that with MRC parameter observation SNR shows no path loss whatever be the number of antenna are considered.

s.no	Scenario	PL parameter		Scenario	PL parameter	
		n	sigma		n	sigma
1	Complex Bedroom	5.5981	1.1176	V2I_NLOS_07deg25dBi_BeamAligning	2.7167	4.1129
2	Complex Bedroom	5.5981	1.1176	V2I_NLOS_07deg25dBi_ no BeamAligning	6.2019	6.5309
3	Complex Bedroom	5.5981	1.1176	V2I NLOS scenario, 22deg/15dBi antenna and Beam Aligning	2.7092	4.0235
4	Complex Bedroom	5.5981	1.1176	V2I NLOS scenario, 22deg/15dBi antenna and no Beam Aligning	4.7057	4.2088
5	Semicomplex Bedroom	5.2027	1.5851	V2I_NLOS_07deg25dBi_BeamAligning	2.7167	4.1129
6	Semicomplex Bedroom	5.2027	1.5851	V2I_NLOS_07deg25dBi_ no BeamAligning	6.2019	6.5309
7	Semicomplex Bedroom	5.2027	1.5851	V2I NLOS scenario, 22deg/15dBi antenna and Beam Aligning	2.7092	4.0235
8	Semicomplex Bedroom	5.2027	1.5851	V2I NLOS scenario, 22deg/15dBi antenna and no Beam Aligning	4.7057	4.2088

I. CONCLUSION

The purpose of this work is to provide a path loss model for mmWave transmissions in a use-case scenario. path loss exponent and shadowing factor parameter are generated for analysis of diversity and sensitivity. These path loss values can be obtained via measurements using channel sounders and various antennas, or can be estimated with a ray tracer.

The work also plots the path loss values and the curves for the model, as soon as it extracts the path loss exponent and the standard deviation of the shadowing factor. A secondary plot shows the distribution of path loss values that represents the mechanism of estimating the shadowing factor value.

The input contains path loss values obtained with the "Wireless InSite" ray tracer by Remcom.

The "PL model" uses 6 path loss files for the indoor scenario and 4 files for the outdoor scenario for analysis. The indoor scenario refers to a customizable conference room and bedroom in which we can remove furniture and electronic equipment; hence, the names “complex," "semi complex," and "simple." The outdoor Vehicular-to-Infrastructure (V2I) NLOS communications scenario is based on two types of horn antennas and a constantly aligning mechanism between Tx and Rx antenna beams.

The analysis shows that at different scenarios different parameters works for antenna propagation and this helps the one to establish it.

REFERENCE

[1.] W. Q. Wang and Z. Zheng, "Hybrid MIMO and Phased-Array Directional Modulation for Physical Layer Security in mmWave Wireless Communications," in *IEEE Journal on Selected Areas in Communications*.

[2.] R. B. Guo, Y. Cai, M. j. Zhao, Q. Shi, B. Champagne and L. Hanzo, "Joint Design of Beam Selection and Precoding Matrices for mmWave MU-MIMO Systems Relying on Lens Antenna Arrays," in *IEEE Journal of Selected Topics in Signal Processing*.

[3.] S. Zhu, H. Liu, P. Wen and Z. Chen, "A Compact Gain-Enhanced Vivaldi Antenna Array with Suppressed Mutual Coupling for 5G mmWave Application," in *IEEE Antennas and Wireless Propagation Letters*.

[4.] D. Solomitckii *et al.*, "Detailed Interference Analysis in Dense mmWave Systems Employing Dual-Polarized Antennas," *2017 IEEE Globecom Workshops (GC Wkshps)*, Singapore, 2017, pp. 1-7.

[5.] A. Ahmad, M. Zafrullah, M. A. Ashraf and A. A. Khan, "Art of antenna designing for 5G (mmWave) next generation networks," *2017 International Symposium on Wireless Systems and Networks (ISWSN)*, Lahore, 2017, pp. 1-4.

[6.] M. V. C. Caya *et al.*, "Basal body temperature measurement using e-textile," *2017IEEE 9th International Conference on Humanoid, Nanotechnology, Information Technology, Communication and Control, Environment and Management (HNICEM)*, Manila, 2017, pp. 1-4.

[7.] R. Guo, Y. Cai, Q. Shi, M. Zhao and B. Champagne, "Joint design of beam selection and precoding for mmWave MU-MIMO systems with lens antenna array," *2017 IEEE 28th Annual International Symposium on Personal, Indoor, and Mobile Radio Communications (PIMRC)*, Montreal, QC, 2017, pp. 1-5.
[8.] D. Čoja, N. Nešković and A. Nešković, "Channel impulse response estimation using vector network analyzer," *2017 25th Telecommunication Forum (TELFOR)*, Belgrade, 2017, pp. 1-4.
[9.] G. D. Surabhi and A. Chockalingam, "Compact Antenna Spacing in mmWave MIMO Systems Using Random Phase Precoding," *2017 IEEE 86th Vehicular Technology Conference (VTC-Fall)*, Toronto, ON, 2017, pp. 1-5.
[10.] C. Lin and G. Y. Li, "Coordinated Beamforming Training for mmWave and Sub-THz Communications with Antenna Subarrays," *2017 IEEE Wireless Communications and Networking Conference (WCNC)*, San Francisco, CA, 2017, pp. 1-6.
[11.] J. Wang, R. Zhang and J. Yuan, "Novel relative navigation for small satellite formation based on antenna arrays using impulse response," *2017 IEEE Aerospace Conference*, Big Sky, MT, 2017, pp. 1-7.
[12.] H. Foltz, O. Kegege and S. Altunc, "Direction finding using an antenna with direction dependent impulse response," *2016 IEEE International Symposium on Antennas and Propagation (APSURSI)*, Fajardo, 2016, pp. 1857-1858.
[13.] N. González-Prelcic, R. Méndez-Rial and R. W. Heath, "Radar aided beam alignment in MmWave V2I communications supporting antenna diversity," *2016 Information Theory and Applications Workshop (ITA)*, La Jolla, CA, 2016, pp. 1-7.
[14.] H. Moon, T. K. Sarkar and W. Zhao, "Reconstruction of three-dimensional free space radiation pattern using non-anechoic measurements factored by the impulse response of the environment," *2016 IEEE Conference on Antenna Measurements & Applications (CAMA)*, Syracuse, NY, 2016, pp. 1-4.
[15.] S. Sun *et al*., "Investigation of Prediction Accuracy, Sensitivity, and Parameter Stability of Large-Scale Propagation Path Loss Models for 5G Wireless Communications," in *IEEE Transactions on Vehicular Technology*, vol. 65, no. 5, pp. 2843-2860, May 2016.
[16.] J. Schneider, J. Gamec, M. Gamcová and M. Repko, "Alternative antenna measuring methods with use of impulse UWB radar," *2016 26th International Conference Radioelektronika (RADIOELEKTRONIKA)*, Kosice, 2016, pp. 296-299.
[17.] A. T. Mobashsher and A. M. Abbosh, "Compact 3-D Slot-Loaded Folded Dipole Antenna With Unidirectional Radiation and Low Impulse Distortion for Head Imaging Applications," in *IEEE Transactions on Antennas and Propagation*, vol. 64, no. 7, pp. 3245-3250, July 2016.
[18.] N. Rostomyan, A. T. Ott, M. D. Blech, R. Brem, C. J. Eisner and T. F. Eibert, "A Balanced Impulse Radiating Omnidirectional Ultrawideband Stacked Biconical Antenna," in *IEEE Transactions on Antennas and Propagation*, vol. 63, no. 1, pp. 59-68, Jan. 2015.
[19.] Y. Yu, J. Zhang, M. Shafi, P. A. Dmochowski, M. Zhang and J. Mirza, "Measurements of 3D channel impulse response for outdoor-to-indoor scenario: Capacity predictions for different antenna arrays," *2015 IEEE 26th Annual International Symposium on Personal, Indoor, and Mobile Radio Communications (PIMRC)*, Hong Kong, 2015, pp. 408-413.
[20.] T. Dallmann and D. Heberling, "A boundary criterion for the effects of a linear phase center shift onto antenna impulse responses," *2014 Loughborough Antennas and Propagation Conference (LAPC)*, Loughborough, 2014, pp. 114-118.
[21.] T. Dallmann and D. Heberling, "Theoretical Investigation of the Effects of a Linear Phase Center Shift onto Antenna Impulse Responses," in *IEEE Antennas and Wireless Propagation Letters*, vol. 13, pp. 1749-1752, 2014.
[22.] M. Perenzoni, "Measurement of spatial response of CMOS antenna-coupled FET detector at 325GHz," *2014 39th International Conference on Infrared, Millimeter, and Terahertz waves (IRMMW-THz)*, Tucson, AZ, 2014, pp. 1-2.
[23.] N. Rostomyan, A. T. Ott, R. Brem, C. J. Eisner and T. F. Eibert, "A Compact balanced symmetric discone antenna with optimized ultrawideband omnidirectional impulse radiation behavior," *The 8th European Conference on Antennas and Propagation (EuCAP 2014)*, The Hague, 2014, pp. 83-86.
[24.] E. G. Farr, "Antenna impulse response and the generalized antenna scattering matrix," *2013 USNC-URSI Radio Science Meeting (Joint with AP-S Symposium)*, Lake Buena Vista, FL, 2013, pp. 70-70.
[25.] L. Zwirello, L. Reichardt, X. Li and T. Zwick, "Impact of the antenna impulse response on accuracy of impulse-based localization systems," *2012 6th European Conference on Antennas and Propagation (EUCAP)*, Prague, 2012, pp. 3520-3523.